iPhone Lidar Can Accurately Capture Fine-Scale Understorey Vegetation Structure

Broghan Mareighd Erland[a,b]*, Jordan P. Cuff[a], Naomi Jones[b], and Rachel Gaulton[b,a]

[a]*School of Natural and Environmental Sciences, Newcastle University, Newcastle-Upon-Tyne, United Kingdom;*

[b]*Fera Science Ltd, York BioTech Campus, Sand Hutton, York, United Kingdom*

* corresponding author

School of Natural and Environmental Sciences,

Newcastle University, Newcastle Upon Tyne, NE1 7RU, United Kingdom

Email. b.m.erland2@newcastle.ac.uk

Abstract:

Complex vegetation structure increases ecosystem resilience, but fine-scale understorey vegetation is often overlooked in monitoring protocols despite subtle variation impacting overall diversity. iPhone lidar has placed cost effective and portable remote sensing technology in the pockets of researchers, farmers, practitioners, and citizens worldwide to conduct continuous monitoring and improve policy decisions globally. This potential is, however, broadly unmet, particularly for the structural assessment of fine-scale vegetation. Measuring heterogeneity of fine-scale understorey vegetation has typically been untenable; requiring either time-consuming manual techniques, or commercial grade lidar methods which are costly and expertise prohibitive for small areas. iPhone lidar was tested for its ability to precisely and accurately measure a broad range of fine-scale understorey vegetation types across 5 agroforest systems in the United Kingdom, from dense broadleaf understorey to the most challenging sparse graminoid flowers. The entire vertical vegetation profile was evaluated, extending beyond metrics such as maximum height or above ground biomass, justifying the use of methods for a broad range of structural metrics across woodland, grassland, cropland and other ecosystems. Multiple scanning scales (e.g. 1 x 1 m and 2 x 5 m) were assessed and compared to a commercial grade laser scanner, with the experimental design extending analyses through randomization to contextualize results. Scanning scales of 1 x 1 m and 2 x 5 m areas achieved accuracy of 2.68 cm ± 0.01 and 3.36 cm ± 0.01, with detection rates of 79% ± 2.6, and 72% ± 2.0 across the full vertical vegetation profile, respectively. When excluding sparse graminoid flowers, accuracy increased up to 1.31 cm ± 0.01 with a 93% ± 0.01 detection rate. The successful performance of iPhone lidar when measuring fine-scale vegetation structure signifies its potential for a transition towards accessible remote sensing methods to better reflect biodiversity and improve policy decisions.

Keywords: herbaceous layer, laser scanning, remote sensing, vegetation structural complexity, vegetation height

Graphical Abstract:

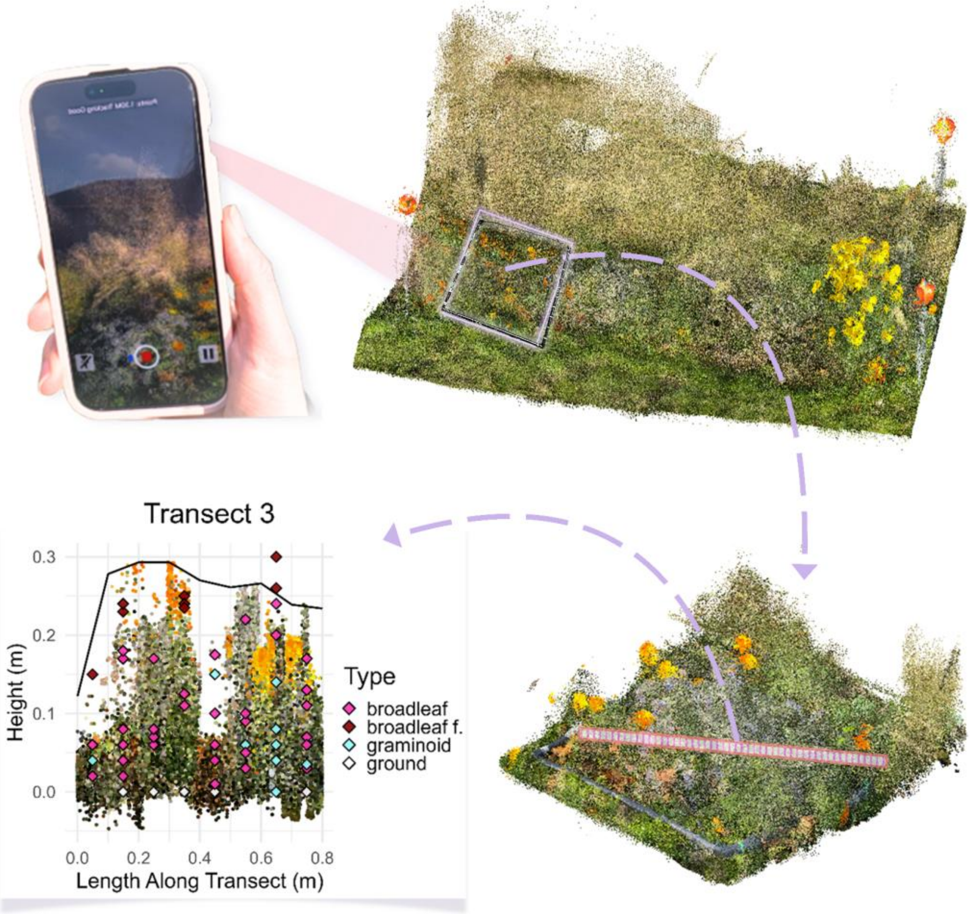

Introduction

Ecological resilience is rooted in diversity (Oliver et al. 2015). Vegetation structure is increasingly recognized as a critical metric of biodiversity and sustainability (Coops et al. 2016; LaRue et al. 2019; Atkins et al. 2023; Maeda et al. 2025; Waddell et al. 2026) as complex three-dimensional vegetation structure increases functional redundancy within plant communities (Coverdale and Davies 2023; LaRue et al. 2019) and microclimate buffering, by moderating changes in carbon, energy, and water processes (Haritika and Negi 2025). This can make ecosystems more resistant to negative feedback loops of biodiversity loss which can help mitigate ecological collapse (Russo et al. 2023). Understorey vegetation, despite being a strong biodiversity indicator (Lenoir et al. 2022), is a commonly overlooked component of vertical complexity across tree-dominated ecosystems (Haritika and Negi 2025; Post et al. 2025). For example, when comparing vegetation complexity across agroforest types in central Europe, understorey was a more pronounced indicator of associated biodiversity services between systems than tree-dominated structural comparisons (Seidel et al. 2021). Furthermore, subtle differences in the heterogeneity of understorey vegetation can determine whether increases in biodiversity indicators are meaningful (Estrada-Carmona et al. 2022; Russo et al. 2023; Marshall et al. 2024; Waddell et al. 2026).

Traditional methods for measuring the structure of ground vegetation are often subjective and laborious, and tend to damage the plants measured (Daughtry 1990; Gayton 2014; Coverdale and Davies 2023), and often poorly reflect the finer scale ecological processes relevant within plots (Gayton 2014; Wallace and Baltzer 2022; Atkins et al. 2023). The point-intercept methods typically used to metricise vegetation quality often omit horizontal complexity and vertical variation (Drezner and Drezner 2021). Given the foundational role of vegetation structure in assessments of wider ecosystem dynamics (Russo et al. 2023; Maeda et al. 2025; Waddell et al. 2026), more comprehensive measurements of understorey vegetation structure across woodland, grassland, cropland, and other ecosystems are required.

Remote sensing technology can measure vegetation using sensors that detect reflected or absorbed energy (Cavender-Bares et al. 2020), and is rapidly advancing in its ability to characterize ecosystem structure using terrestrial, airborne, and satellite monitoring (Irwin et al. 2025; Maeda et al. 2025). Ground-based Terrestrial Laser Scanning (TLS) and Mobile Laser Scanning (MLS) capture vegetation in three-dimensional space by emitting laser pulses to measure X, Y and Z dimensions given rate of returns (Cavendar-Bares 2020). As computational methods advance, ground-based laser scanning methods are poised to provide essential structural and composition metrics to enhance modelling and monitoring of complex ecosystems (Maeda et al. 2025; Irwin et al. 2025). Whilst TLS and MLS have been successfully applied to monitor structural and functional changes in understory vegetation (Eichhorn et al. 2017; Penman et al. 2023; Post et al. 2025), measuring fine-scale vertical heterogeneity of ground vegetation remains complex (Post et al. 2025; Suter et al. 2026), and there are often time lags between the collection of lidar data and paired ecological surveys (Wang et al. 2025). Furthermore, remote sensing technology can at times be inaccessible, largely due to limited access to expertise, knowledge, high costs of equipment and processing software, and/or portability demands of survey-grade instruments (Fassnacht et al. 2024; Maeda et al. 2025; Mmbando 2025).

The incorporation of a lidar sensor into the Apple Inc. iPhone and iPad Pro models since October 2020 (Chase et al. 2022), has placed a cost-effective and portable remote sensing instrument into the pockets of people worldwide. iPhone lidar has a maximum range of 5 m and can attain accuracies of up to ± 1 cm (Treccani et al. 2024; Guenther et al. 2024); however, multiple comparisons have reported accuracies varying from 2 cm to 55 cm, depending on app choice and scanning settings (Chase et al. 2022; Teppati Losè et al. 2022; Askar and Sternberg 2023; Treccani et al. 2024; Guenther et al. 2024; Yanchuk et al. 2025). Building on methods developed for measuring tree parameters in forestry (Tatsumi et al. 2023; Howie and De Stefano 2024; Guenther et al. 2024), but at a more range-applicable level, iPhone lidar could be applied to the measurement structural heterogeneity of fine-scale understorey vegetation. Current iPhone lidar applications for measuring ground vegetation have focused on validating Above-Ground Biomass (AGB) at scales smaller than 0.5 m^2 (Atkins and Blackburn et al. 2025; Dietrich and Elias et al. 2025; Doyle and Raturi 2026). The few studies that included analysis of vertical heterogeneity of the understorey layer solely assessed maximum height (Atkins and Blackburn et al. 2025; Doyle and Raturi 2026). Furthermore, these studies utilized apps that apply a filter or mesh to the lidar points, which can influence results through the introduction of bias and inaccuracies (Teppati Losè et al. 2022, Erland and Gaulton 2026), particularly when scanning plots with low density vegetation (Dietrich and Elias et al. 2025). Studies otherwise indicate promising performance for measurement of vegetation properties. However, the small spatial scale of these existing studies (i.e., 0.25 m^2 or 0.09 m^2) does make them less applicable to most ecological research, which tends to use at least 1 x 1 m quadrats for vegetation assessments. Similarly, the focus of these applications on AGB neglects the important structural characteristics of fine-scale understorey vegetation, accurate measurement of which would present significant value to ecological researchers and practitioners across ecosystem types.

In this study, efficacy of iPhone-based fine-scale understorey vegetation lidar scanning is demonstrated across agroforest types, highlighting its precision, accuracy and interoperability. The use of iPhone lidar could present a cost-effective portable tool to capture fine-scale understorey vegetation and provide access to researchers, practitioners, and citizens to whom alternatives are often inaccessible. This novel application of common technology is poised to expand our understanding of biodiversity by allowing previously unattainable detail to be incorporated into ecological modelling and monitoring.

Methods

Site locations

Sample locations spanned five agroforest systems in the United Kingdom: silvoarable

(52.360370° N, 1.357443° E, Wakelyns Farm, Suffolk), silvopastoral (56.899667° N , -2.549422° W, Glensaugh Farm, James Hutton Institute, Laurencekirk), wood pasture and orchard (55.286586° N, -2.023177° W, Hepple Estate, Northumberland), wood meadow (53.848285° N, -1.048286° W, Three Hagges Woodmeadow Nature Reserve, PlantLife, Yorkshire), and a roadside biodiversity strip (55.045945° N, -1.477593° W, North Tyneside Council, Tyne and Wear). Wakelyns is a wheat-focused working silvoarable agroforestry farm established in 1994, from which three agroforestry areas of the site were sampled: the mature timber and fruit area and two intermediate fruit and nut tree areas planted in 2001. Glensaugh was established in 1988 as an experimental livestock-grazed agroforestry site with the sycamore and Scots pine areas sampled. Sample sites at Hepple included a wood pasture area dominated by mature ash trees originally planted as parkland with a successional scrub area bordering the diverse grassland, which was grazed by cattle and ponies, alongside the Estate's heritage orchard with meadow strips between apple trees. The Three Hagges Woodmeadow was established in 2012 with lowland dry, wet meadows, and mixed woodland species. The roadside biodiversity strip ran parallel to a mature hedgerow, was broadleaf flowering dominant, and closely represents typical municipal biodiversity initiatives.

Scanning equipment

The Apple Inc. iPhone 15 Pro with Sony IMX591 lidar was used for this study and has been shown to have mean accuracies around 2 cm when scanning without a data filter (Erland and Gaulton 2026). The Veesus Ltd. 'Zappcha' app was used for scanning with the 'filter off' option and all other settings otherwise set to default. Comparative Mobile Laser Scanning was obtained via the dedicated GeoSlam Zeb Horizon scanner (Faro Technologies, Inc).

Experimental design: nested scanning levels and reference data

Prior to iPhone lidar scanning, larger sections of the site (~ max 100 m) were scanned using the Zeb Horizon, to allow for a comparison with a dedicated mobile scanning system and for carbon assessment at a later date. Within the Zeb Horizon scanned areas, iPhone lidar data were collected at two main nested levels: a 2 x 5 m plot scan, and a 1 x 1 m quadrat, each placed randomly within the wider plot scan (Figure 1). The 2 x 5 m plot was chosen to ensure all features were within the 5 m range of the iPhone to minimize drift (Bobrowski et al. 2023), and be scanned at a minimum of 1 m distance when walking the plot. In line with similar studies, all plots and quadrats were scanned three times to account for potential scanning issues (Dietrich and Elias et al. 2025).

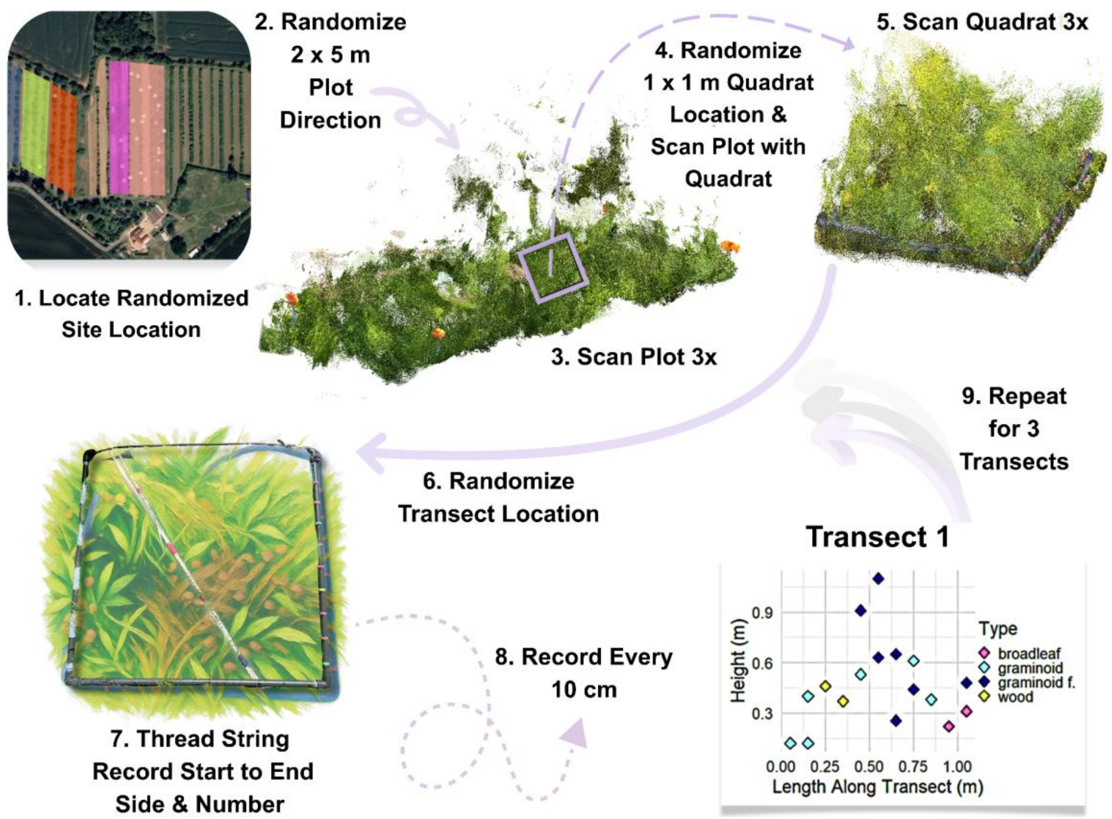

Figure 1. Vegetation scanning workflow. The quadrat panel image (7.) was enhanced in Creately (Cinergix).

Vegetation scanning procedures

Sampling locations were randomized within the different site areas (i.e. mature silvoarable) using Google Earth Engine. Plot direction was randomly selected from the 8 cardinal and intercardinal directions and marked out using 1 m tall orange targets. This was then scanned three times with the iPhone, with scan position initialized from approximately 1 m away from the middle of the 5 m plot edge. All sides were then scanned by walking around the plot, stopping to scan from above at each corner to reduce drift and improve capture of higher features. Quadrat placement was randomized, after which the plot was rescanned for alignment during processing. Scans of quadrats were initialized from 0.5 m away with a 45 degrees downward angle, scanned from all sides and then from above, and repeated three times.

Vegetation field measurements

To obtain the quadrat vegetation reference data, the location of a transect line defined by a string with marked positions every 10 cm, was randomized by side and distance along the side (ten evenly distributed marks), recording the start to end grid coordinates (Figure 2). If the randomization resulted in a length less than 50 cm, it was rerandomized to ensure a minimum of four points were recorded along the transect. The string was then threaded through the vegetation with care taken to minimize damage, and the start and end side and number were recorded (Figure 1.7). Plant functional types and component (e.g., stem, leaf, flower) were recorded alongside heights at every 10 cm mark along the transect string (1.8). The process was repeated so that a total of three transect strings were randomly measured across each quadrat. All randomizations were run in the field using Google's random number generator after each scanning step to minimize bias.

Figure 2. Minimally complex vegetation and the collapsable quadrat designed to allow threading through dense vegetation using a clipped rope side. Holes were drilled every 10 cm along polyvinyl chloride pipe and hooks inserted for threading the measurement string.

Vegetation data categorization

The recorded points were categorized into eight plant functional types: broadleaf, broadleaf flower, graminoid, graminoid flower, mixed (e.g. broadleaf and graminoid), moss, wood and visible ground. The plant component information was also used to categorize data by the likelihood of a return. Graminoid flowers, and graminoid/broadleaf stems were coded as “low” probability; graminoid blades, small broadleaf leaves (<0.5 cm wide) and flowers were coded to “medium”; and thick swards of graminoid plants, average to large broadleaf leaves (>0.5 cm wide), wood and moss were coded as “high”. Ground points were given the “ground” code. Mixed points were coded to the highest category recorded and increased for multiples at the same level (e.g., a graminoid blade and broadleaf stem were coded to “medium”, but a graminoid blade and broadleaf flower measured at the same point would be upgraded to “high”).

Lidar data processing

Using the Veesus Zappcha Xstream Engine CAD plugin, scans which were acquired in the Veesus proprietary. vpc format (Veesus Point Cloud) were loaded into CloudCompare (Version v2.13.2 Kharkiv) (CloudCompare, 2024). Where possible, the first scan was used in the analysis; however, if issues such as large drift or duplicates of a quadrat side occurred within a scan, the next ordered scan was used. Scans that had the “geo-location services” app option turned off were transformed using a Z-plane orientation matrix (Erland and Gaulton 2026). Scans were rotated to have the grey quadrat side parallel with the X plane, segmentation aligned to the quadrat sides using the 'Cross Section' tool, then expanded to a 1.2 m by 1.2 m area for export as .las files and imported into R version 4.4.1 (R Core Team, 2024) using the lidR package (Roussel et al. 2020). Zeb Horizon scans were first processed in GeoSlam Connect (FARO Technologies, Inc.) using the closed loop option and default settings for the "Process-SLAM" workflow (GeoSlam Ltd. 2023), after which the .las files were also imported into CloudCompare.

Once scans were loaded into R, ground points were classified using the cloth simulation filter (Zang et al. 2016) which has previously been applied to data obtained using the Zappcha App (Guenther et al. 2024; Yadav et al. 2023) and outperformed other ground filter methods when applied to high density lidar scans of ground vegetation (Bailey et al. 2022). Given that the focal area is the 1 m by 1 m quadrat, the class threshold was set at 0.01, cloth resolution to 0.250, and the time step, emphasized by Bailey et al. (2022) as a key parameter to reduce when processing dense point clouds, was set to 0.5. Scans were then normalized to the digital terrain model built from the ground classification.

Following the grid coordinates of the quadrat transects were clipped and reorientated to fit the XZ plane using lidR's clip function. As the quadrat had one side with a rope to allow placement through thick vegetation (Figure 2), the quadrat was not always perfectly square (i.e., "normal"), but instead at times a trapezoid with either obtuse (i.e., "wide"), or acute (i.e., "narrow") angles on the opposite rope corners. Coordinates for quadrats that were categorized as "wide" or "narrow" versus "normal" were offset by a shift in (x,y) of (0.1, 0.01) for wide quadrats and (-0.2, -0.02) for narrow quadrats, with differences in shift amounts due to pressure on corners for "wide" quadrats decreasing the angle change. Transects were clipped to a width of 3 cm based on a breakpoint analysis of the influence of clipping width on the percentage of returns and error, along with in-field decisions which had an approximate 1.5 cm inclusion criteria for the distance of an object from each side of the transect string.

Scales of scanning

The nested design of acquiring lidar data allows for comparisons of the same 1 x 1 m quadrat area across devices at different scanning scales (Figure 3). The additional plot scan with the placed quadrat was used to locate the quadrat area in the untouched plot scans. The quadrat from the 2 x 5 m plot was aligned to the 1 x 1 m quadrat using the iterative closest point (ICP) algorithm, a method of registering one point cloud to another using Root Mean Squared Difference computations (Rusinkiewicz and Levoy 2001). Only GeoSlam Zeb Horizon data that could be confidently associated with a specific plot using corresponding targets and/or recognizable features of the sites were used for the analysis. In contrast to the general scanned area, one Zeb Horizon scan was specifically collected by walking the 2 x 5 m plot to directly compare with the iPhone scanning scale.

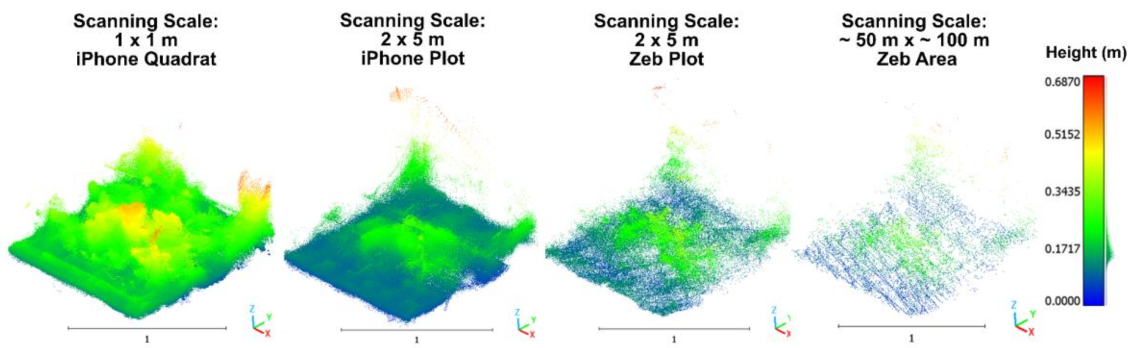

Figure 3. The point cloud and height affects of the different scales of scanning for the same quadrat area in the biodiversity strip using iPhone lidar and the Zeb Horizon.

Height scale ramp was dervied from the 1 x 1 m iPhone quadrat scan scale. The physical quadrat (Figure 2) can be seen in the iPhone quadrat scan.

Lidar metrics

A digital surface model (DSM) with 10 cm resolution was calculated from the maximum lidar points along the transect and compared to the DSM derived from the maximum field-measured reference values and smoothed using locally estimated scatterplot smoothing (LOESS) to minimize bias from the discrete measurements. As values were normalized to the ground DSM estimates represent the vegetation canopy height. To assess the lidar point vertical distribution, the 100th, 95th, 75th, 50th, 25th and 5th percentiles were derived for the lidar and reference transect data. A Kruskal-Wallis non-parametric statistical test was used to assess differences between the lidar and reference data distributions. Transects were further clipped to 1.5 cm radius circles centered around the location of the reference data to assess whether any returns occurred at the expected vegetation point. The percentage of lidar returns, or detection rate, of vegetation measurements was calculated from the number of 1.5 cm radius circles containing at least one point (Figure 4). Return densities (cm^3) were calculated using the number of points within the clipped 1.5 cm radius circles.

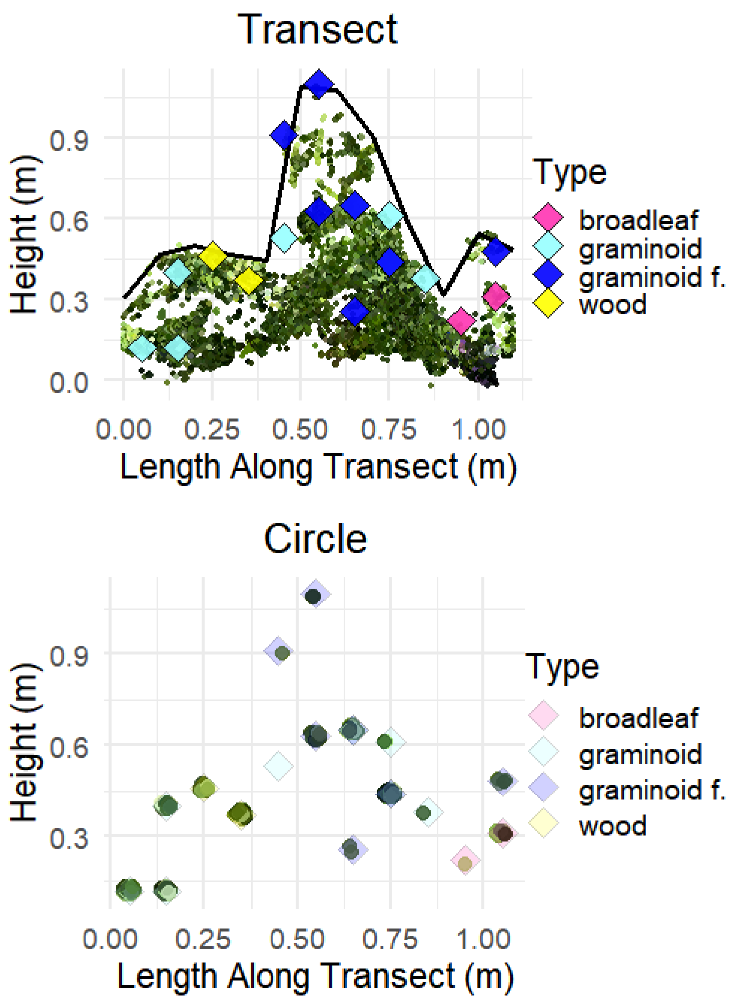

Figure 4. An example of the vertical profile of lidar points (RGB attributed vegetation points), with the digital surface model (black), and field measurements (diamonds, not to scale) for both the transect (top) and 1.5 cm radius clipped circle (bottom).

To estimate scanning error based on the reference measurement locations, a k nearest neighbours' (kNN) analysis was applied to the number of lidar points near each reference point. A breakpoint analysis on overall effect of the choice of k number of neighbours from k = 4 to k = 50 was run using the transect level RMSE values for the whole set of data and by return type (see SI for reasoning behind k value choices).

Relationships between field reference and lidar-derived metrics for the individual quadrats were assessed using a linear mixed effects model in the following form:

Lidar Metric ~ Reference Metric + (Transect | Quadrat Number) + (1 | Site)

The model was also weighted by the inverse number of reference points per transect length to minimize sampling bias due to variations in the number of reference measurements. For low occurrences, such as moss and broadleaf flowers, the site term and, if necessary, the transect line term, were dropped from the model until the number of observations were sufficient for the model. Marginal R^2 and p-values were extracted directly from the model, and the RMSE and MAE were calculated using the residuals from the model outputs. Range relative (rr) values were estimated from the transect-level lidar-derived metrics divided by the range of the reference measurements by transect, then run through the model. Range was used rather than the mean as a relative metric due to the occurrence of multiple near-zero mean values, the variability in the number of reference measurements which biased the mean, and to improve robustness of comparisons across scanning area and devices given the variable vegetation complexity. Parametric bootstrap using 1000 simulations were run to estimate standard error and bias of overall metrics, and semiparametric bootstrap for RMSE standard error estimates.

Comparison of field measurements to random lidar transects

As the three transects for each quadrat were determined using randomization of start to end side and number, the experimental design could be extended to contextualize results and examine metric performance if different lidar transects were randomly extracted for each quadrat compared to the actual lidar transect accuracy for the vegetation reference data. For each 1 x 1 m quadrat, comparisons were run for B = 999 bootstrap randomizations. Transect start-to-end quadrat coordinates were randomized, re-randomizing for lengths less than 50 cm to parallel field methods. Data were analyzed following previous metric methods aside from RMSE standard error estimates which had inherent bias due to the considerably larger sample size of the transects derived from the randomized data (T = 39294), compared to the actual data set (T = 118). As such, bootstraps were run on a subset of 118 transects randomly drawn from the randomized data set (T = 39294), and outputs averaged across 99 different runs of the analysis to determine the standard error.

Results

In total, 40 quadrats were scanned with iPhone 15 Pro lidar and 118 transects analyzed with 2965 measurement points (Table 1; Figure 5). Two transects had to be removed due to the transect coordinates not being recorded. The full process of setting up a plot, scanning at the plot and quadrat level, then measuring vegetation (Figure 1) took, on average, 3 hours per plot largely due to the laborious vegetation measurement process. Five areas that were scanned by the Zeb Horizon were able to be aligned with plot locations using targets and recognizable features to extract the quadrat-level data. Zeb Horizon data were not collected in tandem with the iPhone data at the wood pasture nor wood meadow sites. Growing season varied by site.

Table 1. The number of scanning scales sampled per site given the month along with the percentage of broadleaf (B), broadleaf flower (BF), graminoid (G), graminoid flower (GF), and mixed (M) vegetation types. The wood pasture site was revisited in July and an additional plot with quadrat sampled.

Site	Month in 2024	Number of Quadrats	Number of Plots	Number of Zeb	Percentage of B, BF, G, GF, M %
Silvoarable	June	12	12	2	28, 1, 49, 12, 6
Silvopastoral	August	5	5	1	12, 0,57, 12, 7
Wood pasture	May & July	13	5	NA	11, 1, 48, 21, 11
Wood meadow	August	4	4	NA	33, 12, 33, 6, 12
Heritage Orchard	May	5	3	1	39, 15, 28, 14, 2
Biodiversity Strip	September	1	1	1	49, 21, 23, 1, 1

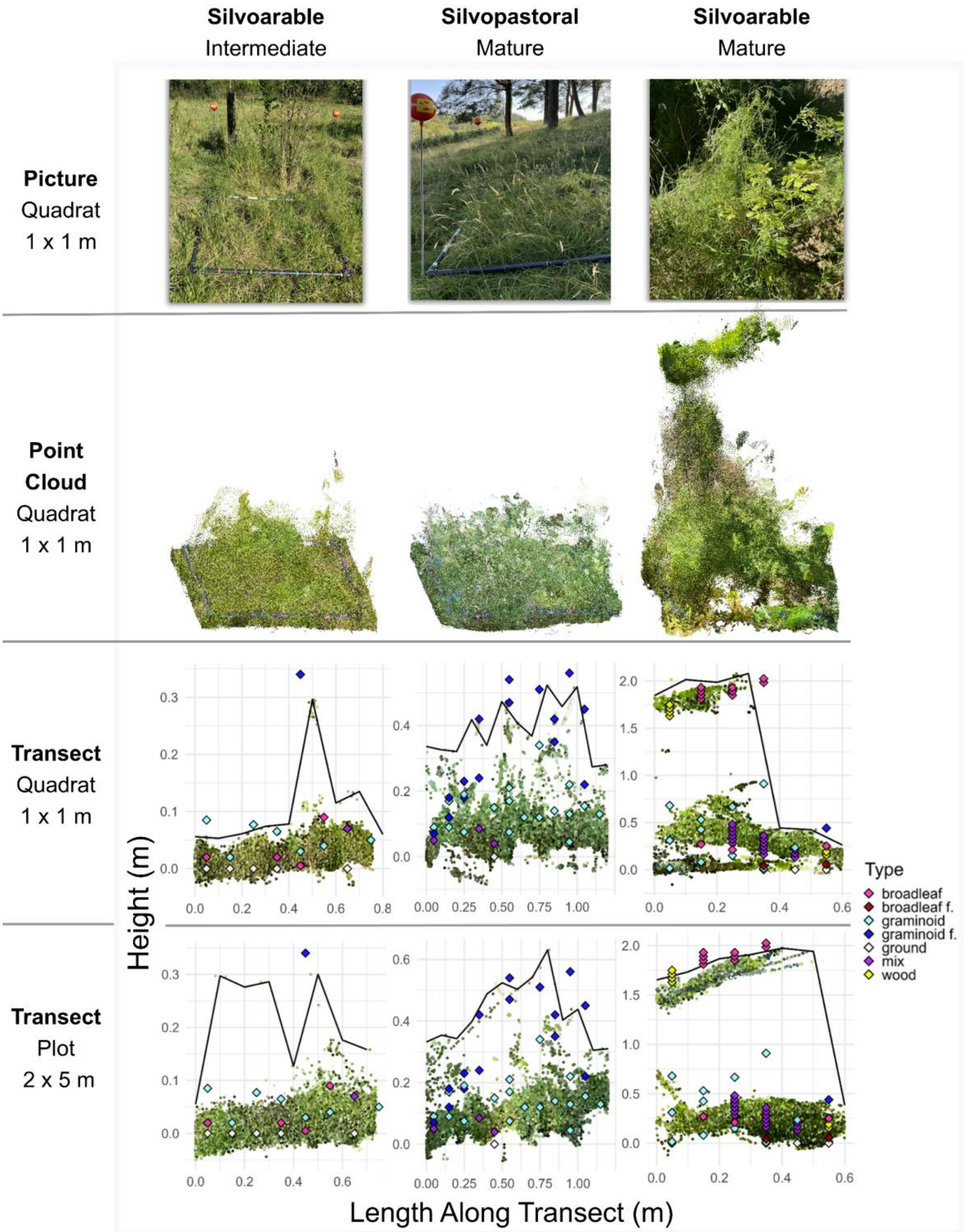

Figure 5. Examples from silvoarable mature and intermediate samples, and a mature silvopastoral site illustrate some of the range in vegetation types and complexity scanned. Pictures and quadrat scale point clouds along with the transect-extracted data are presented at the quadrat and plot scales.

The overall percentage of returns of one or more points occurring within 1.5 cm of a vegetation measurement, hereafter 'detection rate', when excluding graminoid flowers from the analysis was 82.5% ± 1.4 for the quad scan scale, and 68.8% ± 2.5 for plot scan scale (Table 2). Expectedly, due to the low density and movement when measuring, graminoid flowers had low detection rates and low accuracy for both scales of scanning. Error estimates are most appropriate for return types where the number of nearest neighbours (k) is less than the mean density. Ground measurements consistently had the highest detection rate across both the quadrat (95%) and plot (81%) scan scale, which provides additional confidence in iPhone lidar scanning methods. Measurements with mixed vegetation types recorded had a high detection rate and accuracy.

Table 2. For each measured return, the return type, scanning scale, mean detection rates and mean point densities from a lidar return within 1.5 cm of a vegetation measurement are given. Upper and lower bounds of the calculated RMSE and MAE are given for 4 and 50 nearest neighbours (k).

Return Type	Scan Scale	Detection Rate within 1.5 cm	Mean Points within 1.5 cm	RMSE (cm) (k = 4 – k = 50)	MAE (cm) (k = 4 – k = 50)
Overall:	Quad	79 %	39	(2.41 – 3.29)	(1.36 – 2.06)
	Plot	72 %	18	(3.09 – 4.23)	(1.69 – 2.61)
High	Quad	91 %	48	(1.10 – 1.63)	(0.56 – 1.03)
	Plot	82 %	19	(1.41 – 2.24)	(0.80 – 1.42)
Medium	Quad	80 %	38	(1.55 – 2.38)	(0.89 – 1.49)
	Plot	67 %	18	(2.66 – 3.25)	(1.58 – 2.26)
Low	Quad	56 %	14	(3.67 – 4.50)	(2.47 – 3.24)
	Plot	51 %	11	(4.97 – 6.09)	(3.16 – 4.33)
Ground	Quad	96%	127	(0.59 – 0.78)	(0.31 – 0.53)
	Plot	74 %	43	(1.23 – 1.68)	(0.69 – 1.03)
Broadleaf	Quad	91 %	50	(0.99 – 1.53)	(0.50 – 0.95)

	Plot	85 %	19	(1.33 – 2.18)	(0.80 – 1.38)
Broadleaf Flower	Quad	84 %	19	(2.35 – 2.93)	(1.35 – 1.80)
	Plot	74 %	7	(1.91 – 2.29)	(1.38 – 1.67)
Graminoid	Quad	75 %	32	(1.91 – 2.56)	(1.13 – 1.72)
	Plot	67 %	17	(2.91 – 3.55)	(1.74 – 2.45)
Graminoid Flower	Quad	48 %	10	(4.17 – 5.22)	(2.91– 3.79)
	Plot	35 %	7	(5.13 – 6.31)	(3.24 – 4.41)
Mix	Quad	93 %	56	(1.00 - 1.45)	(0.62 – 0.91)
	Plot	87 %	27	(1.01 – 1.48)	(0.62 – 0.93)
Moss	Quad	100 %	120	(0.08 – 0.14)	(0.06 – 0.11)
	Plot	78 %	60	(0.18 – 1.28)	(0.12 – 0.65)
Wood	Quad	85 %	79	(0.99 – 1.89)	(0.55 – 1.07)
	Plot	50 %	9	(2.98 – 5.54)	(2.16 – 4.34)

The change point k value was on average 15, which performs with high accuracy (Table 3, Table S1). Even for graminoid flowers, which performs best given lower k values, the RMSE was still 4.47 cm ± 0.04 for k = 15.

Table 3. Overall average scanning accuracy at the quadrat (1 x 1 m) and plot (2 x 5 m) scanning scales given the use of k = 15 nearest neighbours in analysis.

Return Type	Scan Scale	RMSE (cm) (rrRMSE %)	MAE (cm) (rrMAE %)
Overall:	Quadrat	2.68 ± 0.01 (7.00 ± 0.01)	1.61 ± 0.01 (3.78 ± 0.06)
	Plot	3.36 ± 0.01 (9.80 ± 0.12)	2.00 ± 0.01 (5.65 ± 0.09)

At the quadrat scan scale, the effect of site was marginally insignificant for the k = 15 RMSE derived error (p = 0.05) and detection rate significantly varied across sites

(Figure 6, $p = 0.004$). Vegetation type produces a bimodal distribution of detection rate by site (Figure 6), with the broadleaf-dominated biodiversity strip exhibiting small variation and a unimodal distribution for higher detection rates.

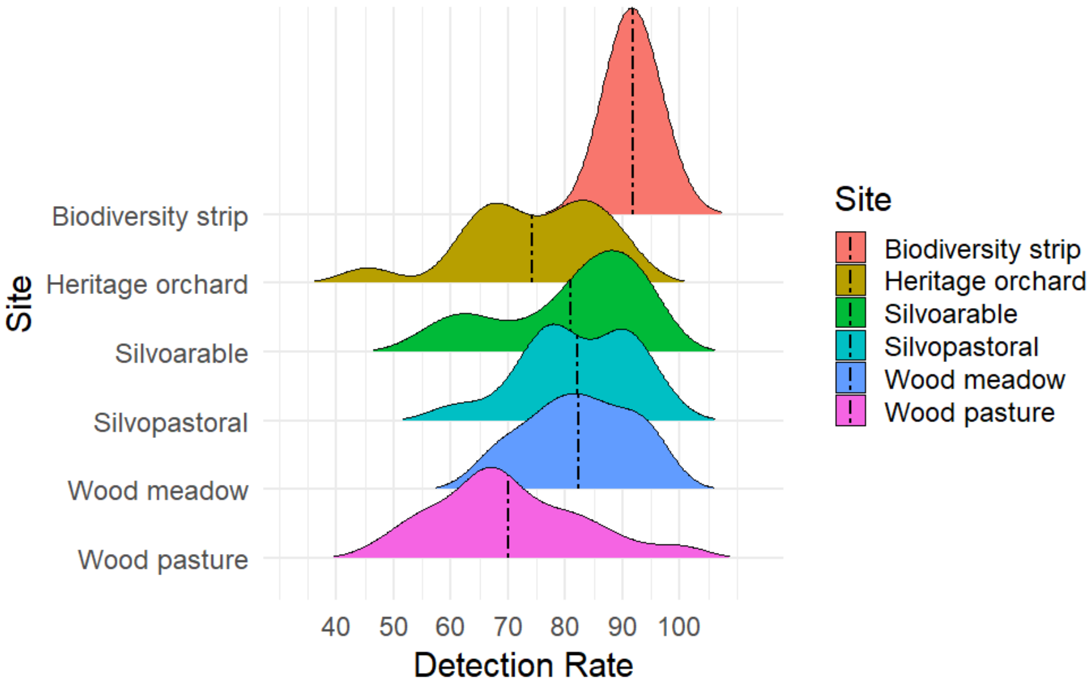

Figure 6. Vegetation type produces a bimodal distribution of detection rates by site. The broadleaf-dominated biodiversity strip exhibited little variation, with a unimodal distribution for a higher detection rate. Mean detection rates by site are represented by a black long dashed vertical line.

Alongside assessing scanning performance of the iPhone lidar at the quadrat and plot scanning levels, performance was also compared to a Zeb Horizon scan of the same plot level, and a Zeb Horizon scan based on a more traditionally representative scanning area. Scanning densities decreased between point clouds for the broadleaf-dominated biodiversity strip given the different devices and scanning scales (Figure 7).

Figure 7. Lidar-derived point cloud data overlaid with the vegetation measurements for the biodiversity strip sample at the scanning scales of iPhone quadrat (1 x 1 m), iPhone plot (2 x 5 m), Zeb Horizon plot (2 x 5 m) and Zeb Horizon area (34 x 130 m). iPhone lidar scans are shown with the associated RGB values and Zeb Horizon with height ramp.

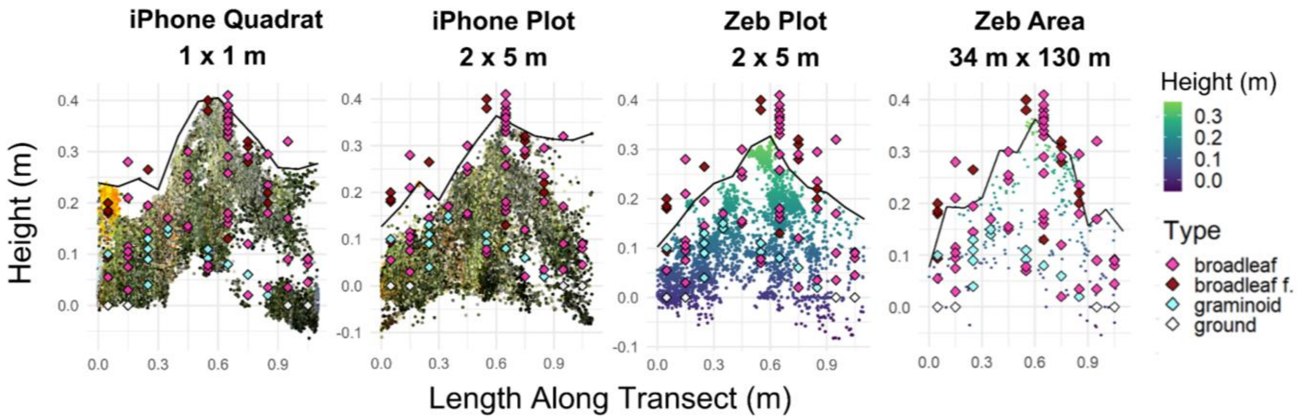

The detection rates when laser scanning fine-scale vegetation using iPhone lidar are markedly higher than those using Zeb Horizon areas scans, as are the point counts, respectively (Table 4). There are no significant distributional differences between the lidar and reference data across all devices and scanning scales (Table 4). The iPhone lidar performed with high accuracy with range relative errors less than 12.5% across scanning scales, and as low as 2.8% for the 1 x 1 m iPhone scans. The quadrat 1 x 1 m scan scale has continued significant and relatively high R^2 values compared to the other devices and scales which taper off as percentiles decrease and vegetation approaches the ground (Table 4). The poor performance of the randomized transect R^2, in contrast to the actual transect estimates, provides further confidence in the accuracy of estimates and the methods used for the validation.

Table 4: Metrics calculated from the transect data given the different devices and scanning scales. For the scanning scales, N = number of quadrats, T = number of

transects, n = number of measurement reference points, and B = number of bootstrap samples. Percentile values in bold are significant at a p-value < 0.05.

Metric	iPhone 1 x 1 m N = 40 T = 118 n = 2965	iPhone 2 x 5 m N = 30 T = 89 n = 2589	Zeb 2 x 5 m N = 1 T = 3 n = 199	Zeb ~50 x 100 m N = 5 T = 15 n = 535	Randomized 1 x 1 m B = 999 N = 40 T = 39294 n = 987012
Average Transect Point Count	65110	19508	2314	390	59445
Detection Rate	79% ± 2.6	72 % ± 2.0	69 %	26 % ± 5.5	60 % ± 3.0
Kruskal-Wallis Test p-value	0.127 ± 0.06	0.144 ± 0.03	0.878	0.498 ± 0.02	0.131 ± 0.04
Canopy Height rrRMSE	28.8 % ± 1.0	35.9 % ± 2.7	17.9 %	37.7 % ± 9.2	42.2 % ± 6.2
Canopy Height rrMAE	23.5 % ± 0.9	29.4 % ± 2.5	15.0 %	30.3 % ± 7.6	35.6 % ± 5.2
KNN rrRMSE %	(5.6 – 9.2)	(7.9 –12.5)	(15.9–25.1)	(12.5 – 20.0)	(10.8 – 14.5)
KNN rrMAE %	(2.8 – 5.4)	(4.2 –7.7)	(10.3–18.7)	(8.0 – 14.3)	(6.0 – 8.9)
100th Percentile: R^2 (rRMSE %)	**0.980± 0.007** (28.7 ± 6.7)	**0.969± 0.013** (39.4 ± 5.3)	**0.998** (4.1)	**0.795± 0.154** (40.0 ± 13.3)	~ 0 ± 0.493 (32.5 ± 6.2)
95th Percentile: R^2 (rRMSE %)	**0.983 ± 0.005** (27.2 ± 6.4)	**0.909 ± 0.044** (27.0 ± 4.8)	0.380 (24.0)	**0.760 ± 0.160** (52.2 ± 23.8)	0.002 ±0.487 (36.8 ± 5.9)
75th Percentile: R^2 (rRMSE %)	**0.861 ± 0.069** (29.4 ± 5.3)	**0.921 ± 0.036** (35.4 ± 5.0)	0.817 (10.4)	**0.877 ± 0.196** (41.4 ± 20.1)	~ 0 ± 0.488 41.7 ± 7.0)
50th Percentile: R^2 (rRMSE %)	**0.664 ± 0.168** (24.7 ± 4.2)	**0.850 ± 0.069** (53.8 ± 8.5)	0.840 (10.0)	**0.724 ± 0.283** (55.6 ± 20.2)	~ 0 ± 0.486 (45.4 ± 8.0)
25th Percentile: R^2 (rRMSE %)	**0.746 ± 0.122** (35.9 ± 6.1)	**0.282 ± 0.352** (82.1 ± 13.9)	0.612 (21.6)	0.128 ± 0.247 (68.7 ± 25.2)	0.002 ± 0.477 (58.0 ± 8.6)
5th Percentile: R^2 (rRMSE %)	**0.639 ± 0.169** (64.1 ± 10.4)	**0.080 ± 0.456** (116.1± 18.4)	0.981 (40.2)	0.001 ± 0.226 (139.6± 60.2)	~ 0 ± 0.458 (82.7 ± 10.4)

Discussion

iPhone lidar can accurately scan understorey vegetation with similar, or better, performance compared to traditional commercial grade lidar methods such as the Zeb Horizon scanner. Analysis of 118 transects from 40 quadrats across 5 different agroforest systems generated highly accurate vegetation structural data across different spatial scales. The accuracy of results was similar to previous forestry applications (i.e., diameter at breast height of large trees; Gollob et al. 2021; Guenther et al. 2024; Howie and De Stefano 2024), with higher accuracy than other comparison studies that used apps with filtering features for point clouds (Chase et al. 2022; Teppati Losè et al. 2022; Askar and Sternberg 2023; Guenther et al. 2024; Treccani et al. 2024; Yanchuk et al. 2025). The relative canopy height error was comparable to Atkins and Blackburn's AGB estimates from scanning 0.25 x 0.25 m quadrats across rangelands (29.3% ± 6.2, and 26.6 ± 3.5 for iPad lidar and Zeb Horizon respectively). The maximum height R^2 across a range of vegetation types were 0.980 ± 0.007 and 0.969 ± 0.013 for the 1 x 1 m and 2 x 5 m lidar scanning scales, respectively, and were better than previous studies with R^2 ranging from 0.583 for grass vegetation to 0.95 for an individual broadleaf plant (Doyle and Raturi 2026; Oikawa et al. 2025; Dietrich and Elias et al. 2025). The validation methods of using randomized transects and measuring vegetation layers across a broad range of agroforests, rather than singular sites, experimental plots or pots, surpassed previous studies to show iPhone lidar can accurately capture the full vertical profile of understorey vegetation across ecosystem types.

While minimized wherever possible, the analysis included inevitable sources of measurement error. The reference points themselves, which were collected using adapted point intercept methods, are subject to common human measurement error alongside environmental interference (e.g., movement from wind). Error was estimated to be approximately 10% of the recorded vegetation height (Caratti 2006). For this study, the mean precision error calculated from all measured points is ± 0.3 cm. Scanning in windy conditions was avoided where possible, and vegetation location, particularly for graminoid flowers, was approximated, but locations such as the silvopastoral site on a hillside in Scotland inevitably encountered wind, which affected vegetation position. Parameter tuning also affected error. The transect and circle clip width impacts metrics; for example, increasing the radius from 1.5 cm inevitably increases detection rate. However, some percentile comparisons performed less accurately after the 3 cm breakpoint due to the inclusion of extraneous vegetation and eventually overlap between measurement points would occur. The smaller clipping widths were chosen to increase the precision accompanying the accuracy estimates. The randomization analysis was chosen to sample within the same 1 x 1 m quadrat to illustrate the precision of estimates using the actual transect location compared to the range in estimates from incorrect transect locations. Randomizations comparing to entirely different quadrats with different vegetation types would inevitably have larger accuracy ranges.

Standardizing fitting procedures is a natural next step for iPhone lidar, particularly when applied to understorey vegetation, as there is variability in the choice of apps used, app settings and downstream processing, all of which can greatly impact the accuracy of capturing fine-scale vegetation structure (Trecanni et al. 2024; Erland and Gaulton 2026). For example, Atkins and Blackburn et al. (2025) scanned vegetation with the 3D Scanner App using a 2 m scan depth and 0.5 cm voxel size, then voxelized scans to 1 p/0.5 cm^3 in CloudCompare and additionally applied a segmentation algorithm to reduce noise and statistical outliers further. Applying a filter or mesh to iPhone lidar will most likely cause finer details that are attributed to the variation in vegetation to be lost rather than reduce scanning noise. Ground normalizing procedures could also be refined to handle the range in point cloud density produced from the scanning scale (e.g., quadrat scale scans averaged 96% ground returns compared to 74% for plot scale scans).

Given that the point cloud data from the iPhone lidar has associated RGB-D values, the natural extension of this work is to study RGB-derived indices. In a controlled laboratory environment, 15 RGB-derived spectral indices were calculated from iPhone lidar RGB-D data and used to estimate leaf nitrogen content with relative root mean square errors as low as 6-15% (Harikumar et al. 2025). Atkins and Blackburn et al. (2025) used multiple regression techniques to explore the link with spectral data when predicting AGB but found a weak relationship ($R^2 = 0.19$). It is hypothesized that improved scanning methods and platforms may improve these results. Additionally, the intensity of return strength associated with each 3-dimensional measurement collected from iPhone lidar has also yet to be explored when scanning vegetation, and the fusion of it with other structural metrics may provide additional novel insights from scans.

Along with expanding metrics from methods, new applications for estimating fine-scale vegetation structural complexity using iPhone lidar could improve governmental biodiversity regulations globally. For example, given the mandated Biodiversity Net Gain regulations across the United Kingdom (DEFRA 2022; DEFRA 2025), there has been criticism of the use of metrics biasing action-based outcomes towards improvement that benefits agriculture rather than overall biodiversity increase (Elmiger et al. 2023; Marshall et al. 2024). Habitat heterogeneity is not well represented in the current metrics used to assess change. This is likely due to the difficulty in capturing the vegetation complexity that increases overall biodiversity, particularly for grassland and woodland (Marshall et al. 2024). Structural complexity is a foundational fixture of ecological complexity (Russo et al. 2023), and having several metrics, with minimal time lags between measurements, to feed into a multifaced framework may be the best approach to assess biodiversity (Waddell et al. 2026). iPhone lidar in the hands of researchers, farmers, and citizen science supporters, could help aid continuous monitoring and improve estimates of habitat heterogeneity while better reflecting ecosystem complexity.

Crucially, the use of iPhone lidar increases the accessibility to remote sensing methods to measure fine-scale understorey vegetation across woodland, grassland, cropland and other ecosystems. Those with limited funds can use previously cost-prohibitive technology which often also requires specialised software to process the data that is collected. Given its lightweight portability, iPhone lidar also increases accessibility to those with disabilities where the weight of commercial equipment tends to create barriers. By introducing cost effective methods for improving diversity assessments, already limited specialized equipment and expert resources could be reallocated to target measurements where the scale of iPhone lidar is restrictive, further increasing the quality of the data that is being collected and used to inform policy. Furthermore, it is easily deployed in landscapes where terrain can constrain the amount of equipment brought by researchers, facilitating remote applications. iPhone lidar provides pocket-sized laser scanning technology to accurately obtain understorey vegetation structure at scales previously inaccessible to many researchers, practitioners and the general population.

Creative Commons Licenses

CRediT Roles

Broghan M. Erland: Conceptualization, Data curation, Formal analysis, Funding acquisition, Investigation, Methodology, Project administration, Resources, Software, Validation, Visualization, Writing – original draft, Writing – review & editing

Jordan P. Cuff: Conceptualization, Supervision, Writing – review & editing.

Naomi Jones: Conceptualization, Funding acquisition, Supervision, Writing – review & editing.

Rachel Gaulton: Conceptualization, Funding acquisition, Resources, Supervision, Writing – review & editing.

Acknowledgments

The authors thank Wakelyns owners David Wolfe and Amanada Illing, Dr. Scot Ramsey of the James Hutton Institute, Mary Gough and the Hepple Estate, The Woodmeadow Trust and PlantLife, and North Tyneside Council's Richard Martin for access to sites. Much thanks to field assistants Pari Balu, Kearti Mondair, and John Schindler for assistance recording data at local sites; and particular acknowledgement and appreciation to Dawna Erland and Retd Major Richard Erland for their work acquiring data and support during lengthy fieldwork at Wakelyns, and Glensaugh respectively.

Funding details

This work was supported by the Institute for Agri-Food Research and Innovation (IAFRI), a joint venture between Newcastle University and Fera Science Ltd., UK; by a Newcastle Overseas Research Scholarship (NUORS) from Newcastle University; and by the Natural Sciences and Engineering Research Council of Canada (NSERC) (PGS D - 578446 - 2023).

Disclosure statement

No potential conflict of interest was reported by the author(s).

Data availability statement

The data supporting the validation of methods are deposited on Zenodo and will be made publicly available upon acceptance of the manuscript.

References

Askar, Cigdem, and Harald Sternberg. 2023. "Use of Smartphone Lidar Technology for Low-Cost 3D Building Documentation with iPhone 13 Pro: A Comparative Analysis of Mobile Scanning Applications." *Geomatics* 3 (4): 563–79. https://doi.org/10.3390/geomatics3040030.

Atkins, David H., Ryan C. Blackburn, Daniel C. Laughlin, Margaret M. Moore, and Andrew J. Sánchez Meador. 2025. "Handheld Lidar Sensors Can Accurately Measure Aboveground Biomass." *Ecosphere* 16 (6): e70232. https://doi.org/10.1002/ecs2.70232.

Atkins, Jeff W., Parth Bhatt, Luis Carrasco, et al. 2023. "Integrating Forest Structural Diversity Measurement into Ecological Research." *Ecosphere* 14 (9): e4633. https://doi.org/10.1002/ecs2.4633.

Bailey, Gene, Yingkui Li, Nathan McKinney, Daniel Yoder, Wesley Wright, and Hannah Herrero. 2022. "Comparison of Ground Point Filtering Algorithms for High-Density Point Clouds Collected by Terrestrial LiDAR." *Remote Sensing* 14 (19): 4776. https://doi.org/10.3390/rs14194776.

Bobrowski, Rogério, Monika Winczek, Karolina Zięba-Kulawik, and Piotr Wężyk. 2023. "Best Practices to Use the iPad Pro LiDAR for Some Procedures of Data Acquisition in the Urban Forest." *Urban Forestry & Urban Greening* 79 (January): 127815. https://doi.org/10.1016/j.ufug.2022.127815.

Cavender-Bares, Jeannine, John A. Gamon, and Philip A. Townsend. 2020. *Remote Sensing of Plant Biodiversity*. Springer International Publishing. https://doi.org/10.1007/978-3-030-33157-3.

Chase, Payton, Kianna Clarke, Audrey Hawkes, Shabnam Jabari, and Jakov Jakus. 2022. "Apple IPhone 13 Pro LiDAR Accuracy Assessment for Engineering Applications." *Transforming Construction with Reality Capture Technologies*, August 19, 2022: The Digital Reality of Tomorrow. https://doi.org/10.57922/TCRC.645.

Coops, Nicholas C., Piotr Tompaski, Wiebe Nijland, et al. 2016. "A Forest Structure Habitat Index Based on Airborne Laser Scanning Data." *Ecological Indicators* 67 (August): 346–57. https://doi.org/10.1016/j.ecolind.2016.02.057.

Coverdale, Tyler C., and Andrew B. Davies. 2023. "Unravelling the Relationship between Plant Diversity and Vegetation Structural Complexity: A Review and Theoretical Framework." *Journal of Ecology* 111 (7): 1378–95. https://doi.org/10.1111/1365-2745.14068.

Daughtry, Craig S. T. 1990. “Direct Measurements of Canopy Structure.” *Remote Sensing Reviews* 5 (1): 45–60. https://doi.org/10.1080/02757259009532121.

Dietrich, Peter, Melanie Elias, Stanley Harpole, Christiane Roscher, and Jan Bumberger. 2025. “Advancing Plant Biomass Measurements: Integrating Smartphone-based 3D Scanning Techniques for Enhanced Ecosystem Monitoring.” *Methods in Ecology and Evolution* 16 (8): 1723–32. https://doi.org/10.1111/2041-210X.70084.

Doyle, Steven, and Ankita Raturi. 2026. “Proximal Sensing of Horticultural Crops with Mobile Device LiDAR.” *Smart Agricultural Technology* 13 (March): 101799. https://doi.org/10.1016/j.atech.2026.101799.

Drezner, Taly Dawn, and Zvi Drezner. 2021. “Informed Cover Measurement: Guidelines and Error for Point-intercept Approaches.” *Applications in Plant Sciences* 9 (9–10): e11446. https://doi.org/10.1002/aps3.11446.

Eichhorn, Markus P., Joseph Ryding, Martin J. Smith, Robin M. A. Gill, Gavin M. Siriwardena, and Robert J. Fuller. 2017. “Effects of Deer on Woodland Structure Revealed through Terrestrial Laser Scanning.” *Journal of Applied Ecology* 54 (6): 1615–26. https://doi.org/10.1111/1365-2664.12902.

Elmiger, By Noëmi, Robert Finger, Jaboury Ghazoul, and Sergei Schaub. 2023. “Biodiversity Indicators for Result-Based Agri-Environmental Schemes – Current State and Future Prospects.” *Agricultural Systems* 204 (January): 103538. https://doi.org/10.1016/j.agsy.2022.103538.

Erland, Broghan M., and Rachel Gaulton. 2026. “A Comparison of Lidar Accuracy across iPhone Models, with Implications for Reproducibility and Cross-Study Comparison.” *Remote Sensing Letters*, ahead of print. https://doi.org/10.1080/2150704X.2026.2720055.

Estrada-Carmona, Natalia, Andrea C. Sánchez, Roseline Remans, and Sarah K. Jones. 2022. “Complex Agricultural Landscapes Host More Biodiversity than Simple Ones: A Global Meta-Analysis.” *Proceedings of the National Academy of Sciences* 119 (38): e2203385119. https://doi.org/10.1073/pnas.2203385119.

Fassnacht, Fabian Ewald, Joanne C. White, Michael A. Wulder, and Erik Næsset. 2024. “Remote Sensing in Forestry: Current Challenges, Considerations and Directions.” *Forestry: An International Journal of Forest Research* 97 (1): 11–37. https://doi.org/10.1093/forestry/cpad024.

Gayton, Don. 2014. “Grassland and Forest Understory Vegetation Monitoring: An Introduction to Field Methods.” *Journal of Ecosystems and Management* 14 (3). https://doi.org/doi.org/10.22230/jem.2013v14n3a173.

GeoSlam Ltd. 2023. “GeoSLAM Connect Software Guide 2.3.” https://knowledge.faro.com/Software/GeoSlam/GeoSLAM_Connect/User_Guide_for_GeoSLAM_Connect.

Gollob, Christoph, Tim Ritter, Ralf Kraßnitzer, Andreas Tockner, and Arne Nothdurft. 2021. “Measurement of Forest Inventory Parameters with Apple iPad Pro and

Integrated LiDAR Technology." *Remote Sensing* 13 (16): 3129. https://doi.org/10.3390/rs13163129.

Guenther, Matthew, Muditha K. Heenkenda, Dave Morris, and Brigitte Leblon. 2024. "Tree Diameter at Breast Height (DBH) Estimation Using an iPad Pro LiDAR Scanner: A Case Study in Boreal Forests, Ontario, Canada." *Forests* 15 (1): 214. https://doi.org/10.3390/f15010214.

Harikumar, Aravind, Itamar Shenhar, Miguel R. Pebes-Trujillo, et al. 2025. "Harnessing Smartphone RGB Imagery and LiDAR Point Cloud for Enhanced Leaf Nitrogen and Shoot Biomass Assessment - Chinese Spinach as a Case Study." *Frontiers in Plant Science* 16 (August): 1592329. https://doi.org/10.3389/fpls.2025.1592329.

Haritika, and A. K. Negi. 2025. "The Underestimated Role of Understory Vegetation Dynamics for Forest Ecosystem Resilience: A Review." *Plant Ecology* 226 (7): 763–87. https://doi.org/10.1007/s11258-025-01529-7.

Howie, Noah A., and Andrea De Stefano. 2024. "Measuring Tree Diameter Using LiDAR Equipped iPad: An Evaluation of ForestScanner and Arboreal Forest Applications." *Forest Science* 70 (4): 304–10. https://doi.org/10.1093/forsci/fxae017.

Irwin, Liam A. K., Nicholas C. Coops, Katharina Anders, Gottfried Mandlburger, and Lukas Winiwarter. 2025. "Light Detection and Ranging of Natural Systems." *Nature Reviews Methods Primers* 5 (1): 76. https://doi.org/10.1038/s43586-025-00446-3.

John F Caratti. 2006. *FIREMON: Fire Effects Monitoring and Inventory System.* Gen. Tech. Rep RMRS-GTR-164-CD. U.S. Department of Agriculture, Forest Service. https://research.fs.usda.gov/treesearch/24062.

LaRue, Elizabeth A., Brady S. Hardiman, Jessica M. Elliott, and Songlin Fei. 2019. "Structural Diversity as a Predictor of Ecosystem Function." *Environmental Research Letters* 14 (11): 114011. https://doi.org/10.1088/1748-9326/ab49bb.

Lenoir, Jonathan, Eva Gril, Sylvie Durrieu, et al. 2022. "Unveil the Unseen: Using LiDAR to Capture Time-lag Dynamics in the Herbaceous Layer of European Temperate Forests." *Journal of Ecology* 110 (2): 282–300. https://doi.org/10.1111/1365-2745.13837.

Maeda, Eduardo Eiji, Benjamin Brede, Kim Calders, et al. 2025. "Expanding Forest Research with Terrestrial LiDAR Technology." *Nature Communications* 16 (1): 8853. https://doi.org/10.1038/s41467-025-63946-6.

Marshall, Cicely A. M., Kristian Wade, Isla S. Kendall, et al. 2024. "England's Statutory Biodiversity Metric Enhances Plant, but Not Bird nor Butterfly, Biodiversity." *Journal of Applied Ecology* 61 (8): 1918–31. https://doi.org/10.1111/1365-2664.14697.

Mmbando, Gideon Sadikiel. 2025. "Harnessing Artificial Intelligence and Remote Sensing in Climate-Smart Agriculture: The Current Strategies Needed for

Enhancing Global Food Security.” *Cogent Food & Agriculture* 11 (1): 2454354. https://doi.org/10.1080/23311932.2025.2454354.

Oikawa, Nozomi, Yuji Nakagawa, Toshiaki Owari, Shinichi Tatsumi, and Satoshi N. Suzuki. 2025. “Utilising LiDAR -equipped iPhone in Forestry: Constructing 3D Models and Measuring Tree Sizes in a Planting Site.” *Ecological Solutions and Evidence* 6 (1): e12399. https://doi.org/10.1002/2688-8319.12399.

Oliver, Tom H., Matthew S. Heard, Nick J. B. Isaac, et al. 2015. “Biodiversity and Resilience of Ecosystem Functions.” *Trends in Ecology & Evolution* 30 (11): 673–84. https://doi.org/10.1016/j.tree.2015.08.009.

Penman, Sandra, Pia Lentini, Bradley Law, and Alan York. 2023. “An Instructional Workflow for Using Terrestrial Laser Scanning (TLS) to Quantify Vegetation Structure for Wildlife Studies.” *Forest Ecology and Management* 548 (November): 121405. https://doi.org/10.1016/j.foreco.2023.121405.

Post, Alanna J., Brieanne Forbes, Zane Cooper, et al. 2025. “Using Handheld Mobile Laser Scanning to Quantify Fine-Scale Surface Fuels and Detect Changes Post-Disturbance in Northern California Forests.” *Ecological Indicators* 172 (March): 113276. https://doi.org/10.1016/j.ecolind.2025.113276.

Roussel, Jean-Romain, David Auty, Nicholas C. Coops, et al. 2020. “lidR: An R Package for Analysis of Airborne Laser Scanning (ALS) Data.” *Remote Sensing of Environment* 251 (December): 112061. https://doi.org/10.1016/j.rse.2020.112061.

Rusinkiewicz, S., and M. Levoy. 2001. “Efficient Variants of the ICP Algorithm.” *Proceedings Third International Conference on 3-D Digital Imaging and Modeling*, 145–52. https://doi.org/10.1109/IM.2001.924423.

Russo, Nicholas J., Andrew B. Davies, Rachel V. Blakey, Elsa M. Ordway, and Thomas B. Smith. 2023. “Feedback Loops between 3D Vegetation Structure and Ecological Functions of Animals.” *Ecology Letters* 26 (9): 1597–613. https://doi.org/10.1111/ele.14272.

Seidel, Dominik, Melissa Stiers, Martin Ehbrecht, Maik Werning, and Peter Annighöfer. 2021. “On the Structural Complexity of Central European Agroforestry Systems: A Quantitative Assessment Using Terrestrial Laser Scanning in Single-Scan Mode.” *Agroforestry Systems* 95 (4): 669–85. https://doi.org/10.1007/s10457-021-00620-y.

Suter, Samantha, Claudine Ah-Peng, Sarah Kabache, Dominik Seidel, Dominique Strasberg, and Delphine Clara Zemp. 2026. “Towards Scaling-Up Three-Dimensional Habitat Structural Measurements with Multi-Sensor Remote Sensing.” Preprint, Ecology, April 23. https://doi.org/10.64898/2026.04.21.719810.

Tatsumi, Shinichi, Keiji Yamaguchi, and Naoyuki Furuya. 2023. “FORESTSCANNER: A Mobile Application for Measuring and Mapping Trees with iPhone and iPad.” *Methods in Ecology and Evolution* 14 (7): 1603–9. https://doi.org/10.1111/2041-210X.13900.

Teppati Losè, Lorenzo, Alessandra Spreafico, Filiberto Chiabrando, and Fabio Giulio Tonolo. 2022. “Apple LiDAR Sensor for 3D Surveying: Tests and Results in the Cultural Heritage Domain.” *Remote Sensing* 14 (17): 4157. https://doi.org/10.3390/rs14174157.

Treccani, Daniele, Andrea Adami, and Luigi Fregonese. 2024. “Assessing the Effectiveness of LiDAR-Based Apps on Apple Devices to Survey Indoor and Outdoor Medium Sized Areas.” *The International Archives of the Photogrammetry, Remote Sensing and Spatial Information Sciences* XLVIII-2/W8-2024 (December): 431–38. https://doi.org/10.5194/isprs-archives-XLVIII-2-W8-2024-431-2024.

UK. DEFRA. 2022. *Department for Environment Food & Rural Affairs: Consultation on Biodiversity Net Gain Regulations and Implementation*. York. https://www.gov.uk/government/consultations/consultation-on-biodiversity-net-gain-regulations-and-implementation.

UK DEFRA. 2025. “Understanding Biodiversity Net Gain.” Department for Environment, Food & Rural Affairs. https://www.gov.uk/guidance/understanding-biodiversity-net-gain.

Waddell, Emily H., Ben Woodcock, Jim Harris, et al. 2026. “Drivers of Complexity in Ecosystem Restoration.” *Journal of Applied Ecology* 63 (4): e70387. https://doi.org/10.1111/1365-2664.70387.

Wallace, Cory A., and Jennifer L. Baltzer. 2022. “Scale-dependent Responses of Understory Vegetation to the Physical Structure of Undisturbed Tundra Shrub Patches.” *Ecosphere* 13 (9): e4218. https://doi.org/10.1002/ecs2.4218.

Wang, Zhengyang, Jenia Singh, and Andrew B. Davies. 2025. “Consistent Patterns of LiDAR-Derived Measures of Savanna Vegetation Complexity between Wet and Dry Seasons.” *Ecological Indicators* 170 (January): 113061. https://doi.org/10.1016/j.ecolind.2024.113061.

Yadav, Y., S. K. P. Kushwaha, M. Mokros, J. Chudá, and M. Pondelík. 2023. “INTEGRATION OF IPHONE LiDAR WITH QUADCOPTER AND FIXED WING UAV PHOTOGRAMMETRY FOR THE FORESTRY APPLICATIONS.” *The International Archives of the Photogrammetry, Remote Sensing and Spatial Information Sciences* XLVIII-1/W3-2023 (October): 213–18. https://doi.org/10.5194/isprs-archives-XLVIII-1-W3-2023-213-2023.

Yanchuk, Oleksandr, Roman Shulgan, Serhii Trokhymets, and Nazarii Sheremet. 2025. “Accuracy Assessment of a Three-Dimensional Model Obtained Using the LiDAR Sensor of the iPhone 13 Pro Max.” *Geodesy and Cartography* 51 (1): 11–17. https://doi.org/10.3846/gac.2025.20797.

Supplemental Material

Various k values were tested: k = 4 as a minimum k value and average point density from graminoid flowers; k = 5 as the most commonly used value in forestry analysis (Chirici et al. 2016), k = 6 as the average square root value derived from the log distribution of the point densities within a circle; k = 10 as the maximum value reported in forestry literature (Chirici et al. 2016) and the in-field intuitive value from processing the circle data; k = 15 as the average square root of the point densities within each circle; k = 30 as a classic central limit theory value; and k = 50 given that iPhone lidar point count is 10-fold denser than typical terrestrial scanning lidar data (Erland et al., in revision; Chirici et al. 2016).

Table S1. Root Mean Squared Error (RMSE) slope and the breakpoint estimated value for each vegetation category and lidar return likelihood.

	Slope: RMSE Increase Per added Neighbour (cm)	k Breakpoint Estimate
Overall	0.028	18.7
High	0.014	18.3
Medium	0.026	19.4
Low	0.047	17.2
Ground	0.008	21.8
Broadleaf	0.015	13.7
Broadleaf Flower	0.021	12.3
Graminoid	0.025	21.8
Graminoid Flower	0.061	16.6
Moss	0.009	6.0
Wood	0.026	17.5
Average Across Vegetation	0.024	15.7